

Maximum Average Entropy-Based Quantization of Local Observations for Distributed Detection*

Muath A. Wahdan and Mustafa A. Altinkaya

Department of Electrical and Electronics Engineering

İzmir Institute of Technology

İzmir, Turkey

muathwahdan@iyte.edu.tr and mustafaaltinkaya@iyte.edu.tr

Abstract

In a wireless sensor network, multilevel quantization is necessary in order to find a compromise between the smallest possible power consumption of the sensors and the detection performance at the fusion center (FC). The general methodology is using distance measures such as J-divergence and Bhattacharyya distance in this quantization. This work proposes a different approach which is based on maximizing the average output entropy of the sensors under both hypotheses and utilizes it in a Neyman-Pearson criterion based distributed detection scheme in order to detect a point source. The receiver operating characteristics of the proposed maximum average entropy (MAE) method in quantizing sensor outputs was obtained for multilevel quantization both when the sensor outputs are available error-free at the FC and when non-coherent M-ary frequency shift keying communication is used for transmitting MAE based multilevel quantized sensor outputs over a Rayleigh fading channel. The simulation studies show the success of the MAE both in the cases of isolated error-free fusion and in the case where the effect of the wireless channel is incorporated. As expected the performance gets better as the level of quantization increases and with six-level quantization it approaches the performance of non-quantized data transmission.

keyword: distributed detection, multilevel quantization, point source, wireless sensor networks.

1 Introduction

Wireless Sensor Networks (WSNs) have come into the spotlight recently due to a major development in the Micro-Electro-Mechanical Systems (MEMS) [1, 2]. The recent development of WSNs have made this field a research focus of intensive researches. The researchers are widely using it in monitoring and

*A preliminary version of this paper was presented in the 27th Signal Processing and Communications Applications Conference (SIU), Sivas, Turkey, 24-26 April 2019.

characterizing large physical environments and for tracing various environmental or physical conditions such as temperature, pressure, wind, and humidity. Apart from these, WSNs have vast fields to be applied in, such as harmful environmental exploration, wildlife monitoring, target tracking and smart cities established based on Internet of Things (IoT) [3–6]. Typically a WSN uses a huge number of comparatively inexpensive and low-energy sensors to collect observations and pre-process the observations. These sensors are generally deployed in the environment. Owing to strict energy and bandwidth restrictions, observations of the sensors are frequently needed to be quantized before transmitting them to a fusion center (FC) where a global decision is made [7,8]. In this work, we concentrate on the distributed detection problem of a WSN and how the local observations are quantized.

The pioneering research on fusion rules was made by Tenney and Sandell [10] and Chair and Varshney [11]. In [10], a detection problem consisting of two sensors and one FC with a fixed fusion rule was considered to show that the optimum local decision rule is the likelihood ratio test (LRT) under the Bayesian criterion. However, the individual thresholds are coupled. Later, in [11], it was shown that the optimum fusion rule at the FC for multiple observations is also a LRT both under the Neyman-Pearson (NP) and the Bayesian criteria. Determining the local decision rules is significantly more complicated. The optimality of LRT for each local decision rule was considered in [12], [13] and [14], by assuming conditional independence of the observations under each hypothesis. But because of the coupling between the LRT thresholds at the local detectors among themselves and with the one at the FC solving the global optimization problem is mathematically complex though not intractable [15]. This complexity suggested determining the thresholds of the local detectors independently, that is, the threshold of each sensor is optimized for fixed decision rules at the other detectors and the FC [16]. The adopted conditional independence assumption in those works produce only locally optimal decisions, but even they become prohibitively complex for large sensor networks and simpler solutions are needed. Additionally, the gain obtained by having more sensor nodes outperforms the gain of getting more information from each sensor in WSNs [16]. For more details on the fusion rules for different network topologies such as parallel, serial and tree topologies consider the literature [17–20].

Optimum quantization levels in the sense of information theoretic criteria for distributed detection systems were presented in [21–25]. In [21], the quantization based on Ali-Silvey distances between two simple hypotheses was investigated. After that, in [22], [23], the divergence was proposed as a distortion measure by considering a class of f-divergence measures which shows that the loss in divergence is quadratic with the quantization step size.

In [24,25], the authors considered that each local detector transmits a multiple-bit decision to the FC. The solution for partitioning the local decision space was derived by maximizing the distance between the mean values of the quantized hypotheses. It was shown that, the global decision performance increases monotonically by increasing the number of partitions at the individual detector. This method is locally optimum in the sense of J-divergence (JD), but it does not necessarily yield a globally optimum solution. Even when four quantization levels are considered, the solution is given by complicated analytic expressions explaining the functional relationships between the detection probability and the false alarm probability of all detectors and their derivatives. In those works, it was assumed that all local sensors are identical NP detectors observing the same signal-to-noise ratio (SNR).

In [26], in order to perform optimum quantization in the sense of mean-error, deflection criterion (DC) and Chernoff information (CI) were defined for distributed detection systems consisting of one FC and multiple sensors by using Bayesian detection criterion. DC and CI pose a nonlinear and non-convex problem, which mostly has more than one extreme. These kinds of optimization criteria are suitable for the case of known SNR where the probability of detection and probability of false alarm are known for each local detector.

Traditional distributed detection systems were developed by assuming an error-free communication between the local detectors and the FC [13], [14]. Applying this theory to WSNs leads to a detection performance loss in case of erroneous channels. Fusion rules for distributed detection systems considering fading channels were first discussed in [27] and later in [28–30] mainly for a binary hypothesis testing whereas M-ary hypothesis testing was considered in [31–34] for binary data transmissions.

Inspiring from quantization of signals using the Maximum Output Entropy (MOE) in [35], we propose an entropy based method by maximizing the average entropy of observations under both hypotheses to determine the quantization intervals at distributed sensors in order to optimize the global binary decision at the FC about the existence of a point source under the NP criterion where sensors observe different signal levels which they do not know. Although maximizing the entropy is a well-known approach, it has not been used in decision problems until now to the best of our knowledge. The most probable reason for this is the widespread acceptance that an information theoretic criterion for decision problems should concentrate on the distance of rival hypotheses. We consider scenarios with non-equivalently important hypotheses, that is why NP criterion is considered to be more suitable compared to probability of error criterion in this work. This paper extends its preliminary version [36] in the following aspects. We compare the proposed method to popular JD [24,25] based method, demonstrate its positively proportional relation with JD, include increased quantization levels resulting in similar performance to non-quantized signalling. Instead of the binary symmetric channel as a simplified model for the channel from the sensors to the FC, we use regular Rayleigh fading channel model for the wireless channel. Additionally, optimal and sub-optimal fusion rules are utilized which are modified from the ones for M-ary hypothesis testing in [34] in order to match the binary hypothesis testing problem with M-ary modulated data transmission.

The remaining part of this paper is organized as follows. First, we formulate the parallel distributed detection problem of a point source including sensor to FC transmissions over a Rayleigh fading channel and various fusion rules in Section 2. Section 3 covers the development of the proposed average entropy based quantization method, the JD based method and their relation. Simulation results are given in Section 4 and conclusions are drawn in Section 5.

Notation: Boldface lower and upper case letters denote vectors and matrices, respectively. The symbol " \sim " stands for "distributed according to", whereas $\mathcal{N}(\mu, \sigma^2)$ denotes Gaussian probability density function (pdf) with mean μ and variance σ^2 . $\mathcal{CN}(\boldsymbol{\mu}, \mathbf{C}_{\bar{y}})$ denotes complex Gaussian pdf with mean vector $\boldsymbol{\mu}$ and covariance matrix \mathbf{C} .

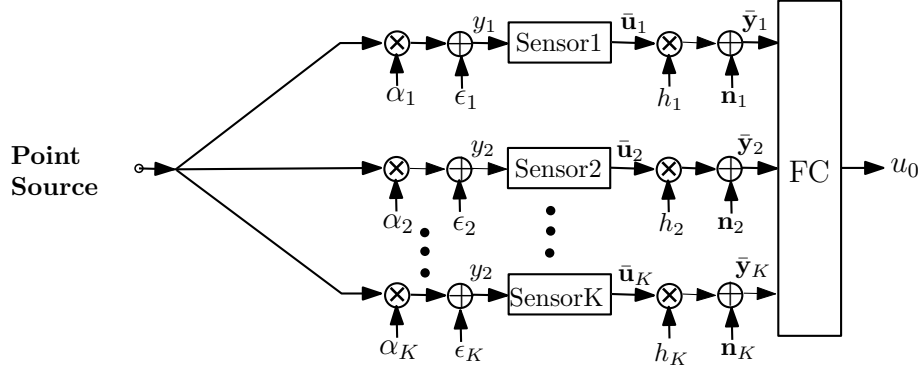


Figure 1: Parallel distributed detection system.

2 System model

A binary hypothesis testing problem has been considered in this work, where a group of K sensors and one FC cooperate to detect the existence of a point source as shown in Figure 1. The hypothesis testing at each sensor node can be described as

$$\begin{aligned}
 &H_0 : y_k = \epsilon_k, \\
 &\text{versus} \\
 &H_1 : y_k = A_k + \epsilon_k,
 \end{aligned} \tag{1}$$

where y_k denotes the observation at the k th sensor and ϵ_k denotes additive white Gaussian noise (AWGN) with variance σ^2 and zero mean. A_k denotes the received signal amplitude which is equal to $\alpha_k A_{\max}$. Each sensor in the range of the point source detects a signal attenuated with a factor of α_k and makes a local decision u_k . The local decision is transmitted through multiplicative channel h_k to the FC where the final decision u_0 is made. In Figure 1, the sensor outputs $\{\bar{\mathbf{u}}_k, k = 1, 2, \dots, K\}$, the AWGNs in the channel from the sensors to the FC $\{\mathbf{n}_k, k = 1, 2, \dots, K\}$ and the received signals $\{\bar{\mathbf{y}}_k, k = 1, 2, \dots, K\}$ are shown as vectors in accordance with the M -dimensional signal model of Frequency Shift Keying (FSK) related modulated signal model, explained in detail in section 2.2.1.

Based on the dispersion pattern over the surveillance zone and the physical characteristics, the phenomenon to be detected can be modeled either as a field source or a point source. A field source is dispersed over the sensor field such as in temperature monitoring. On the other hand, the event is generated by a single point source such as in target detection and fire detection.

2.1 Point source

In this work, we consider a point event source emitting constant power uniformly in all directions. For such a source the signal amplitude received by a sensor will be inversely proportional to the distance from the source. Considering uniformly deployed sensors, only those sensors which are within a circle the radius of which is determined by the sensitivity of the sensors, will receive a signal.

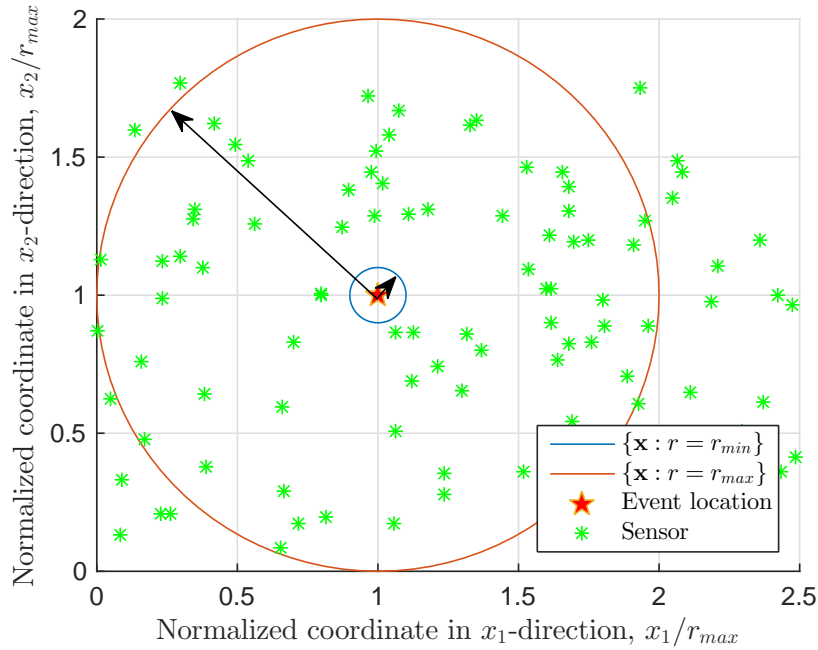


Figure 2: Positions of the event location and uniformly distributed sensors transmitting to the FC.

Let A_{\max} denote the signal amplitude on a circle with radius r_{\min} centered by the event location as shown in Figure 2. We assume that A_{\max} corresponds to the maximum detectable signal level or the saturation level of the sensors and A_{\min} denotes the minimum value of the detectable signal observed at a distance of r_{\max} from the event location. This yields a different and unknown amplitude value for each individual sensor. Assuming there are no sensors in the small circle, the pdf of the normalized signal amplitude, $A_n = A/A_{\max}$, at a sensor will have the form shown in Figure 3 and will be given as:

$$p(A_n) = \frac{1}{A_n \log(L)} \quad (2)$$

where $L = A_{\max}/A_{\min}$ and $\log(\cdot)$ is the natural logarithm. We define the SNR as the ratio between the maximum signal power, A_{\max}^2 , and the noise power, σ^2 . Let us assume that K of the sensors uniformly deployed in the area will be in the fat ring (or punctured disk) described by the radii r_{\min} and r_{\max} . Then, the signal amplitudes at these sensors will be independent and come from the pdf given in (2) in the case of an event. Assuming that the sensor observations are available distortion-free at the FC, i.e. without transmission over a wireless channel, the optimal Bayesian NP detector can be written as:

$$\Lambda(\mathbf{y}) = \frac{\prod_{k=1}^K \int_{A_{\max}/L}^{A_{\max}} p(y_k|H_1; A_k) p(A_k) dA_k}{p(\mathbf{y}|H_0)} \underset{H_0}{\overset{H_1}{\gtrless}} \eta. \quad (3)$$

Since each A_k comes from the independent and identical pdf given in (2), we eliminate the index, k , and

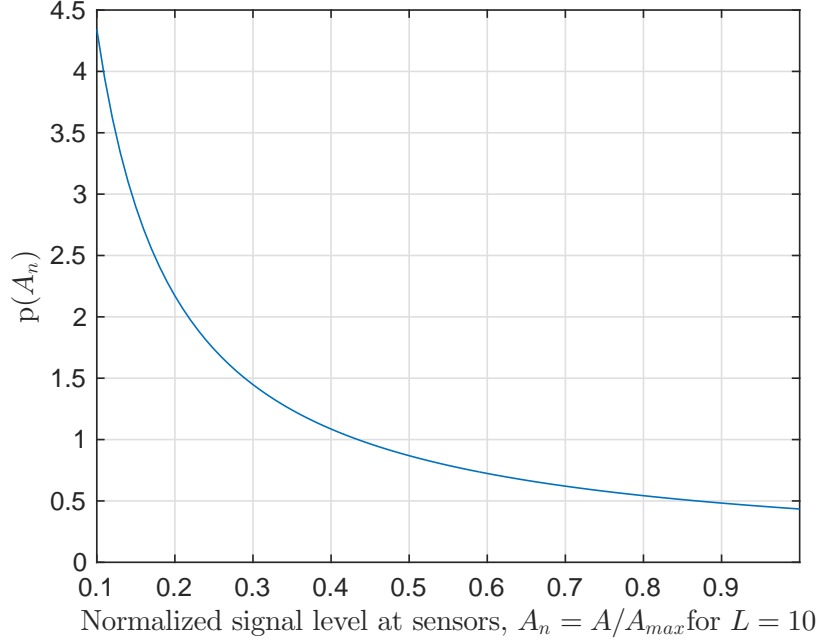


Figure 3: The probability density function of the signal amplitude observed at the sensors, $p(A_n)$.

express the likelihood ratio as

$$\Lambda(\mathbf{y}) = \frac{\prod_{k=1}^K \int_{A_{max}/L}^{A_{max}} \frac{1}{\sqrt{2\pi\sigma^2}} \exp\left(\frac{-(y_k - A)^2}{2\sigma^2}\right) \frac{1}{A \log(L)} dA}{\left(\frac{1}{\sqrt{2\pi\sigma^2}}\right)^K \exp\left(\frac{-\sum_{k=1}^K (y_k)^2}{2\sigma^2}\right)} \underset{H_0}{\overset{H_1}{\geq}} \eta, \quad (4)$$

where $\mathbf{y} = [y_1, y_2, \dots, y_K]$ denotes vector of observations from K sensors.

2.2 Fusion System: Channel Between Sensors and FC

In this section we will investigate the complete model of the sensor to FC communication by using a Rayleigh fading channel model and an M -ary frequency-shift keying (M -FSK) modulation scheme where M different symbols are transmitted by a carrier wave of different frequency for each different symbol. M -FSK is a suitable modulation scheme for low power low data rate data transmission as preferred by majority of the sensor device equipment. In [34], the error probability when the detectors perform FSK modulation was minimized when training symbol transmit power is zero. Accordingly, non-coherent demodulation of M -FSK was adopted in this paper. Additionally, in order to concentrate on the fusion of sensor data with non-identical signal levels, we considered the case of no channel, i.e. when error-free sensor outputs are available at the FC, which we called as direct data transmission (DDT). Once data from the sensors are at the FC, an equal gain fusion rule is applied for every different type of sensor transmissions to FC since the relative reliability of sensor outputs are not evaluated.

2.2.1 Fading channel

In this subsection, the problem of fusing the data transmitted over a fading channel has been considered, as shown in Figure 1. The FC has only information on the channel statistics. Non-coherent M -FSK modulation is employed for transmitting data to the FC. Let \mathbf{u}_k denote the M -FSK modulated symbol at sensor k , where $\mathbf{u}_k \in \{\mathbf{e}_m, m = 1, \dots, M\}$ and \mathbf{e}_m is an $M \times 1$ column vector, all elements of which except the m th one are zero. We refer to the transmit power of the data symbol as P_d . Assuming M -dimensional signal model for representing the orthogonal channels of M -FSK modulation scheme between the detectors and the FC [34] simplifies the analysis. Then, the output of the channel which is corresponding to detector k at the FC can be given as:

$$\begin{aligned}\bar{\mathbf{y}}_k &= \sqrt{P_k} h_k \mathbf{u}_k + \mathbf{n}_k \\ &= h_k \bar{\mathbf{u}}_k + \mathbf{n}_k\end{aligned}\quad (5)$$

where P_k represents the received power which is a function of P_d , the wavelength, the path loss exponent and the distance between detector k and the FC [34] and it describes the effect of large scale fading. The channel noise is denoted as \mathbf{n}_k which is a zero mean complex Gaussian vector $\mathbf{n}_k \sim \mathcal{CN}(0, \sigma_n^2 I)$, where I is an $M \times M$ identity matrix. The complex channel coefficient h_k in (5) is modeled as $h_k \sim \mathcal{CN}(0, 1)$ which can be also represented as $h_k = \alpha_k e^{j\phi_k}$, where α_k represents the amplitude with Rayleigh distribution and ϕ_k represents the phase with uniform distribution. We adopt NP criterion to find the optimal and a sub-optimal fusion rule at the FC in order to obtain a global decision $u_0 \in \{H_0, H_1\}$ as follows.

- (i) The optimal fusion rule for the independent and identically distributed (i.i.d.) vectors, $\bar{\mathbf{y}}_k, k = 1, 2, \dots, K$, is defined as follows:

$$\log \Lambda(\mathbf{Y}) = \log \frac{p(\mathbf{Y}|H_1)}{p(\mathbf{Y}|H_0)} = \log \prod_{k=1}^K \frac{p(\bar{\mathbf{y}}_k|H_1)}{p(\bar{\mathbf{y}}_k|H_0)} \underset{H_0}{\overset{H_1}{\geq}} \eta, \quad (6)$$

where \mathbf{Y} is the matrix composed by row-wise stacking column vectors $\mathbf{y}_k, k = 1, \dots, K$.

Expanding $p(\bar{\mathbf{y}}_k|H_1)$ and $p(\bar{\mathbf{y}}_k|H_0)$ in (6) over the M -level sensor decisions we obtain

$$\log \Lambda(\mathbf{Y}) = \sum_{k=1}^K \log \left(\frac{\sum_{m=1}^M p(\bar{\mathbf{y}}_k|\mathbf{u}_k(m)) p(\mathbf{u}_k(m)|H_1)}{\sum_{m=1}^M p(\bar{\mathbf{y}}_k|\mathbf{u}_k(m)) p(\mathbf{u}_k(m)|H_0)} \right) \underset{H_0}{\overset{H_1}{\geq}} \eta, \quad (7)$$

where K represents the number of sensors and M represents the number of quantization levels at each local sensor. The conditional density $p(\bar{\mathbf{y}}_k|\mathbf{u}_k(m))$ in (7) is a complex multi-variate Gaussian density, $\bar{\mathbf{y}}_k \sim \mathcal{CN}(0, \mathbf{C}_{\bar{\mathbf{y}}})$, $\mathbf{C}_{\bar{\mathbf{y}}}$ represents the diagonal matrix with entries $\mathbf{C}_{\bar{\mathbf{y}}}(j, j) = \sigma_n^2$ for $j \neq m$ and $\mathbf{C}_{\bar{\mathbf{y}}}(j, j) = P_k \sigma_h^2 + \sigma_n^2$ for $j = m$, where $j = 1, \dots, M$. We can prove that $p(\bar{\mathbf{y}}_k|\mathbf{u}_k(m))$ equals to

$$\frac{1}{\sqrt{\pi^M \det |\mathbf{C}_{\bar{\mathbf{y}}_m}|}} \exp \left\{ -(\bar{\mathbf{y}}_k - \boldsymbol{\mu})^H \mathbf{C}_{\bar{\mathbf{y}}_m}^{-1} (\bar{\mathbf{y}}_k - \boldsymbol{\mu}) \right\}. \quad (8)$$

The values of $p(\mathbf{u}_k(m)|H_1)$ represent the probability masses under hypothesis H_1 , which are estimated as:

$$\overline{p}_m^{H_1} = \int_{A_{\max/L}}^{A_{\max}} p_m^{H_1}(A_n) p(A_n) dA_n, \quad (9)$$

where $p_m^{H_1}(A_n)$ represents the probability mass under H_1 as shown in Figure 4 for an observed signal level A_n which is the mean of the Gaussian signal.

The values of $p(\mathbf{u}_k(m)|H_0)$ represent the probability masses under hypothesis H_0 :

$$p(u_k(m)|H_0) = p_m^{H_0}. \quad (10)$$

Figure 4 shows a possible partitioning of a pdf under hypothesis H_i , $i = 1, 2$ and the probability masses for $M = 4$ corresponding to the areas under the pdf between successive thresholds.

- (ii) A sub-optimal fusion rule can be derived as follows: In (7) we see both the effects of fading channel and the local detection outputs in order to achieve the optimal performance. A direct alternate could be used as a sub-optimal fusion rule by separating this into two-steps. First, $\bar{\mathbf{y}}_k$ is used to infer about the local detector by applying the maximum likelihood (ML) estimate as an intermediate decision, \hat{u}_k , and then, the optimum fusion rule based on \hat{u}_k is applied:

$$\hat{u}_k = \operatorname{argmax}_m \boldsymbol{\theta}_m, \quad (11)$$

where $\boldsymbol{\theta}_m$ is given as

$$\boldsymbol{\theta}_m = p(\bar{\mathbf{y}}_k | \mathbf{u}_k(m)). \quad (12)$$

We can re-write (8) as in [34]

$$p(\bar{\mathbf{y}}_k | \mathbf{u}_k(m)) = \frac{1}{\sqrt{\pi^M \det |\mathbf{C}_{\bar{\mathbf{y}}_m}|}} \exp\left(\frac{P_k \sigma_h^2 |\bar{y}_k(m)|^2}{\sigma_n^2 (\sigma_h^2 + \sigma_n^2)}\right) \prod_{j=1}^M \exp\left(\frac{|\bar{y}_k(j)|^2}{\sigma_n^2}\right). \quad (13)$$

By substituting (13) in (11) after eliminating the terms which are irrelevant to m , we can re-write (11) as

$$\hat{u}_k = \operatorname{argmax}_m \exp\left(\frac{P_k \sigma_h^2 |\bar{y}_k(m)|^2}{\sigma_n^2 (\sigma_h^2 + \sigma_n^2)}\right), \quad (14)$$

where $m = 1, \dots, M$. Note that $|\bar{y}_k(m)|^2$ in (14) denotes the squared envelopes of M cross-correlators corresponding to non-coherent FSK detection.

The final decision rule is given as

$$u_0 = \sum_{k=1}^K \hat{u}_k \underset{H_0}{\overset{H_1}{\geq}} \eta. \quad (15)$$

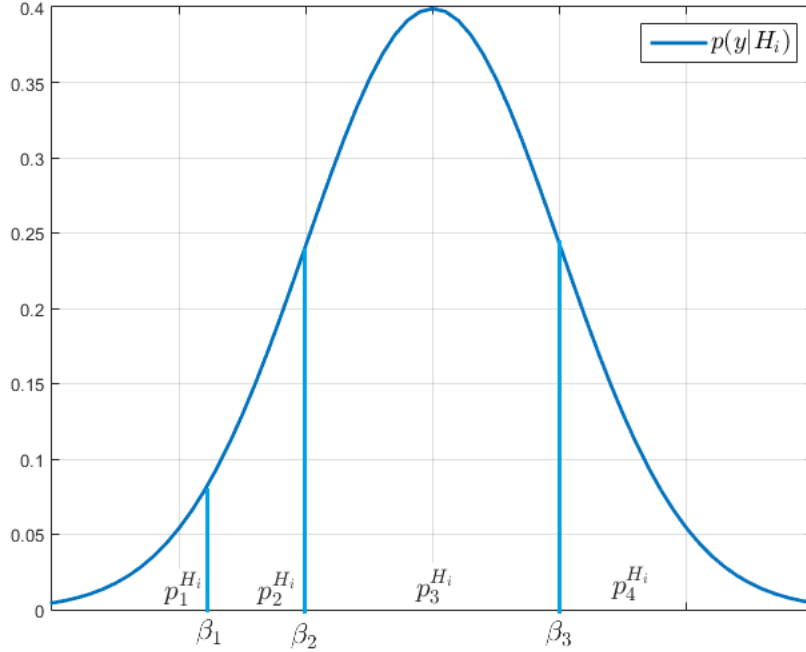


Figure 4: A partitioning of the pdf for the observations at each sensor for 4-level quantization.

3 Quantizer Design

It is aimed to make a global decision at the FC under the NP criterion. Let us assume that each sensor will only make a single observation and will transmit this observation to the FC. Then, sensors will make i.i.d. observations under H_0 and none of the sensors can estimate the signal level under H_1 . Consequently, there is no information at the sensors in order to use different quantization thresholds under H_1 . So, it is reasonable to use identical quantization thresholds at each sensor irrespective of their distance to the event location since it cannot be estimated. Definitely, the choice of the quantization thresholds affects the performance which makes it desirable to choose the quantization thresholds which maximizes the system performance. This paper proposes maximum average entropy (MAE) method, that is, determining the quantization thresholds at the sensors in the way to maximize the average entropy of the discrete information collected at the FC under both hypotheses without considering the effects of the succeeding wireless channel. To the best of our knowledge all of the entropy based quantizers for detection problems are some distance measures [21, 26]. The proposed MAE method differs from them in that it maximizes the transmitted information corresponding to both of the underlying probability mass functions (pmfs) jointly.

The optimum detector at the FC is based on likelihood ratios as given in (4). Equivalently, one can use log-likelihood (logarithm of likelihood) ratios and the log-likelihood ratio for the k th sensor with an unknown signal amplitude can be calculated by using the expected value of the signal amplitude, \bar{A} ,

as follows:

$$\log(\Lambda) = -\frac{\bar{A}^2}{2\sigma^2} + \frac{\bar{A}}{\sigma^2} y_k. \quad (16)$$

The linear (or more appropriately affine) transformation of observations in (16) to log-likelihood ratios is irrelevant in entropy based quantization because that kind of transformation only results in translation and scaling of the underlying pdfs and will preserve the resulting probability masses corresponding to a vector of thresholds (such as β_1 , β_2 and β_3 in Figure 4). Consequently, the sensors will transmit quantized observation signal to the FC. A common information based criterion for determining the quantization thresholds is the maximum JD (MJD) method which was used in the case of constant signal level at sensors formerly [24]. We will first explain these criteria and subsequently the relation between them.

3.1 Maximum Average Entropy Method

An intuitive idea to have an optimum performance at the FC is to maximize the entropy under both hypotheses which we call as MAE method [36]. So, we propose to determine the quantization intervals at the sensors as resulting in MAE under both hypotheses. The entropy of a quantized sensor output can be calculated based on the partitioning of the observation pdf at each sensor as shown in Figure 4. In this figure, the number of quantization intervals is 4. For a general number of M quantization intervals, there will be $M - 1$ thresholds, $\{\beta_1, \beta_2, \dots, \beta_{M-1}\}$, and M partitions with corresponding probability masses of observations $\{p_1^{H_i}, p_2^{H_i}, \dots, p_M^{H_i}\}$ where $i = 0, 1$. Under H_i , the entropy of the observation can be estimated as

$$\hat{F}_{H_i} = \hat{E} \left(- \sum_{m=1}^M p_m^{H_i} \log_2(p_m^{H_i}) \right) \text{bit}. \quad (17)$$

The expectation, $\hat{E}(\cdot)$, is with respect to the distribution of the K sensors and in the special case of the scenario described in Figure 2, this distribution is uniform in the sensing range of the sensors defined by a circle within a radius of r_{\max} from the event location. $\mathbf{p}_M^{H_0} = [p_1^{H_0}, p_2^{H_0}, \dots, p_M^{H_0}]$ denotes the vector of these probability masses, i.e. the probabilities of the partitions. In practice, an estimate of this expectation is obtained by averaging the information of the sensors over the distribution of the sensor locations and AWGN realizations which is called a histogram method [37]. Figure 5 shows the entropy function \hat{F}_{H_0} , \hat{F}_{H_1} and $\hat{F}_{\text{av}} = \frac{1}{2}(\hat{F}_{H_0} + \hat{F}_{H_1})$ for binary quantization. For M -ary quantization, $\boldsymbol{\beta}_M^* = [\beta_1^*, \beta_2^*, \dots, \beta_{M-1}^*]$ denotes the vector of optimum quantization thresholds in the sense of MAE which is found as

$$\boldsymbol{\beta}_M^* = \underset{\boldsymbol{\beta}_M}{\text{argmax}} \hat{F}_{\text{av}}. \quad (18)$$

Optimal quantization thresholds for binary quantization corresponds to the maximum of \hat{F}_{av} as shown in Figure 5 which is $\beta_2^* = 0.093$. In a similar way, we can estimate the optimal thresholds for 3-level quantization to be $\boldsymbol{\beta}_3^* = [-0.341 \quad 0.528]$ as shown in Figure 6 in terms of equal level contours. Similarly, the optimum thresholds are $\boldsymbol{\beta}_4^* = [-0.367 \quad 0.195 \quad 0.835]$ in the case of 4-level quantization and $\boldsymbol{\beta}_6^* = [-1.08 \quad -0.572 \quad -0.060 \quad 0.4513 \quad 0.963]$ for 6-level quantization.

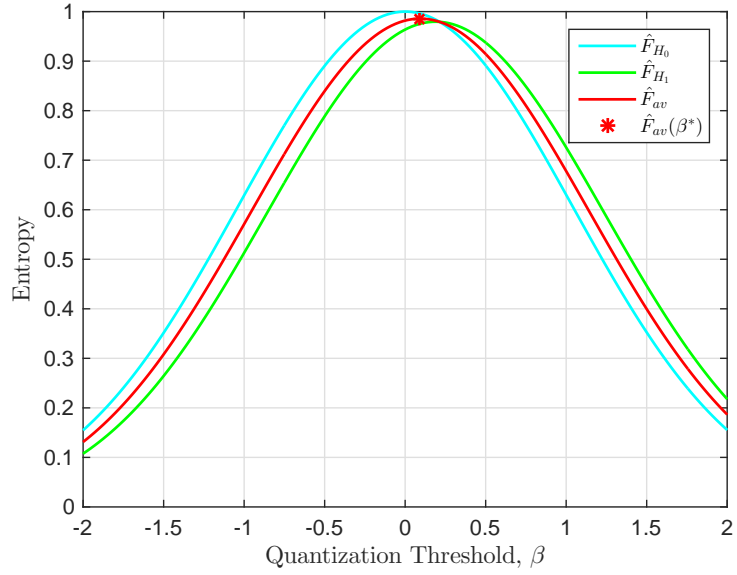


Figure 5: The entropy functions \hat{F}_{H_0} , \hat{F}_{H_1} and \hat{F}_{av} for binary quantization.

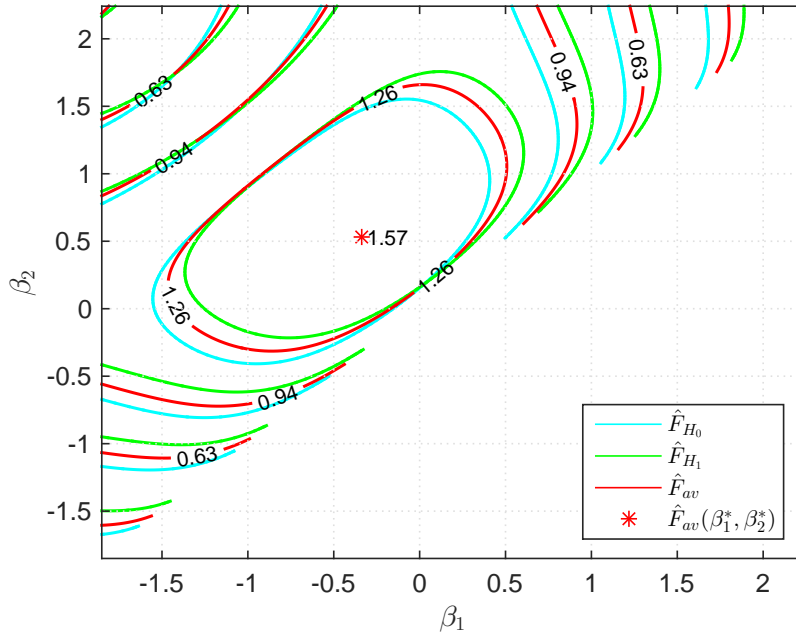


Figure 6: The entropy functions \hat{F}_{H_0} , \hat{F}_{H_1} and \hat{F}_{av} for three level quantization.

3.2 Maximum J-divergence Method

JD can be written in terms of the relative entropy for discrete probability distributions P and Q observed under the two hypotheses H_0 and H_1 , respectively, as follows:

$$J = D_{KL}(P||Q) + D_{KL}(Q||P), \quad (19)$$

where the relative entropy between two pmfs $P(x)$ and $Q(x)$ is given as follows:

$$D_{KL}(P||Q) = \sum_{x \in \chi} P(x) \log_2 \left(\frac{P(x)}{Q(x)} \right), \quad (20)$$

where χ denotes the alphabet of the pmfs for P and Q . In our context, JD measures the distributional distance or dissimilarity between the distributions of the observations under two hypotheses H_0, H_1 and this can be used to find the local thresholds. The choice of local thresholds facilitates the design of local detectors which in turn determines the performance of the whole system. An estimate of the expected value for the JD can be obtained by averaging the contribution to the JD over the distribution of sensor locations and noise realizations as performed for entropy of the observations in (17) and can be written as:

$$\hat{J} = \hat{E} \left(\sum_{m=1}^M \left[p_m^{H_1} \log_2 \left(\frac{p_m^{H_1}}{p_m^{H_0}} \right) - p_m^{H_0} \log_2 \left(\frac{p_m^{H_0}}{p_m^{H_1}} \right) \right] \right). \quad (21)$$

It is obvious that \hat{J} as specified by (21) is a function of the probability masses corresponding to the partitions of the pdf. For M -ary quantization, $\boldsymbol{\beta}_M^\circ = [\beta_1^\circ, \beta_2^\circ, \dots, \beta_{M-1}^\circ]$ denotes the JD optimized vector of quantization thresholds which can be given as

$$\boldsymbol{\beta}_M^\circ = \underset{\boldsymbol{\beta}_M}{\operatorname{argmax}} \hat{J}. \quad (22)$$

Optimal quantization thresholds correspond to the maximum of \hat{J} which is found to be $\beta_2^\circ = 0.17$ for binary quantization as shown in Figure 7. In a similar way, we can estimate the optimal thresholds for 3-level quantization to be $\boldsymbol{\beta}_3^\circ = [-0.444 \quad 0.784]$ as shown in Figure 8. Similarly, the optimal thresholds are $\boldsymbol{\beta}_4^\circ = [-0.725 \quad -0.699 \quad 0.6559]$ in the case of 4-level quantization and $\boldsymbol{\beta}_6^\circ = [-6.19 \quad -0.572 \quad -0.0603 \quad 0.9628 \quad 6.59]$ for the 6-level quantizations.

3.3 Relation of MAE and MJD Methods

In this subsection we will demonstrate that both of the information based criteria, namely, MAE and MJD, maximize similar quantities in showing that they are positively proportional. Let us first express $D_{KL}(P||Q)$ given in (20) as follows:

$$D_{KL}(P||Q) = \underbrace{\sum_{x \in \chi} P(x) \log_2 \left(\frac{1}{Q(x)} \right)}_{R_1} + \underbrace{\sum_{x \in \chi} P(x) \log_2(P(x))}_{-F_{H_0}} \geq 0. \quad (23)$$

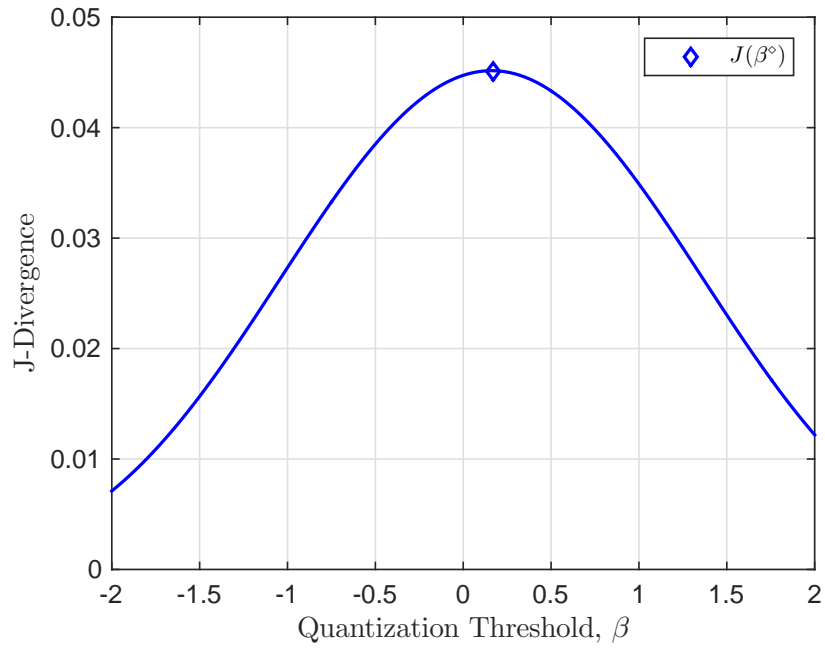


Figure 7: The J-divergence for binary quantization.

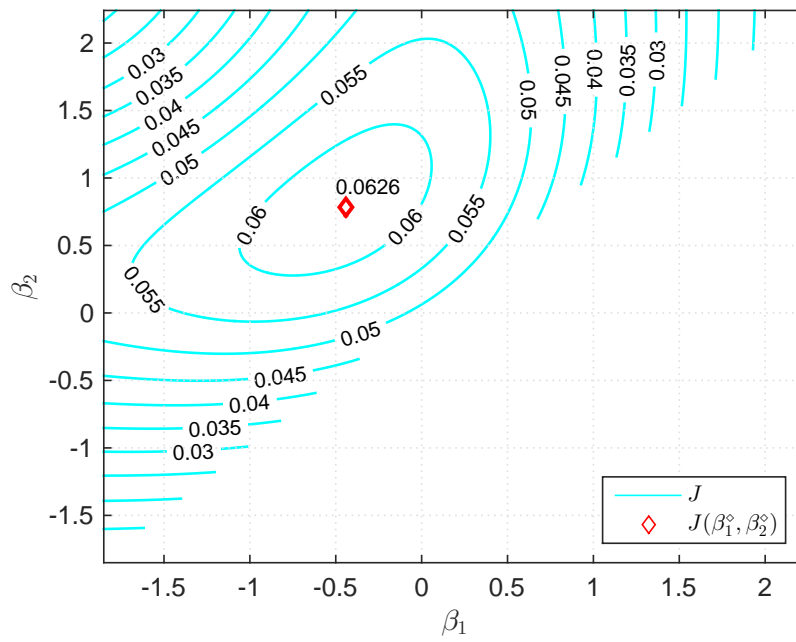


Figure 8: The J-divergence for three level quantization.

The equality holds only when $P = Q$. Similarly,

$$D_{KL}(Q||P) = R_2 - F_{H_1} \geq 0, \quad (24)$$

where $R_2 = \sum_{x \in \mathcal{X}} Q(x) \log_2 \left(\frac{1}{P(x)} \right)$. Substituting (23) and (24) into (19)

$$J = R_1 + R_2 - (F_{H_0} + F_{H_1}) \geq 0. \quad (25)$$

Then, defining $D_{KL}(P||Q) = c_1 F_{H_0}$ and $D_{KL}(Q||P) = c_2 F_{H_1}$, we can re-write the JD in (25) to show that there is a proportionality relation between the JD and the average entropy (AE):

$$\begin{aligned} J &= c_1 F_{H_0} + c_2 F_{H_1} \\ &= \min\{c_1, c_2\} \underbrace{(F_{H_0} + F_{H_1})}_{2F_{av}} + c_3 \end{aligned} \quad (26)$$

with

$$c_3 = \begin{cases} (c_1 - c_2)F_{H_0} & \text{for } c_1 \geq c_2, \\ (c_2 - c_1)F_{H_1} & \text{for } c_1 \leq c_2 \end{cases}. \quad (27)$$

Obviously $c_i \geq 0$ for $i = 1, 2$ and 3. This means that AE and JD are positively proportional.

4 Simulation Results

Monte Carlo simulations have been performed in order to evaluate the detection performance for the proposed method at SNR= 0 dB for $K = 25$ transmitting sensors and $L = A_{\max}/A_{\min} = 10$. First we have performed simulations using the direct data transmissions (DDT) method, that is assuming the sensor outputs are available error-free at the FC for both MAE and MJD methods. Then, a Rayleigh fading channel is considered to show the channel effect on the performance of our proposed quantization method, MAE.

4.1 Binary Direct Data Transmission

In Figure 9, the Receiver Operating Characteristics (ROC), that is probability of detection (p_d) versus probability of false alarm (p_{fa}), curves are plotted for the cases of using the quantization intervals from MAE and MJD methods for the binary data transmission and the corresponding non-quantized data transmissions. The K th root quantization, which uses the K th root of the global probability of false alarm $p_{fa} = 0.1$ to find pmf $\tilde{p}_2^{H_0} = 0.89$ at each sensor, is also provided for the comparison with the proposed method, MAE. K th root method corresponds to setting the false alarm threshold at the FC to a single "one" coming from any of K sensors. In this figure, we observe a slightly better performance of MAE-based method compared to MJD-based one. Each of them perform much better compared to the trivial K th root method which is supplied as an obvious lower bound. Additionally, we observe that they are clearly inferior to the non-quantized case which shows that there is quite a large space for gain in using higher levels of quantization.

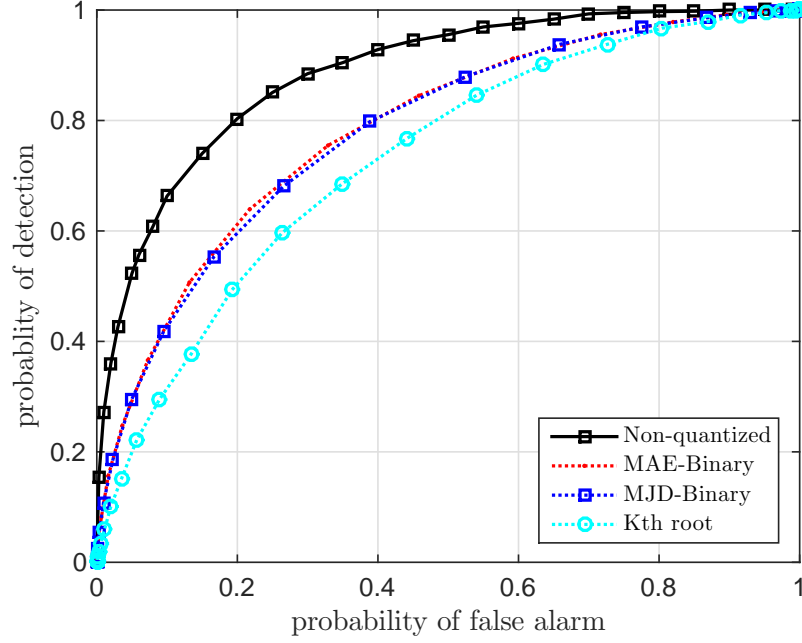


Figure 9: Comparison between the ROC curves obtained using MAE, MJD and Kth root methods for binary and Gaussian (non-quantized) DDT.

4.2 Performance of MAE and MJD with Multilevel Quantization

The simulation performances for the three-level, four-level and six-level quantizations by using the MAE and MJD methods are also obtained for DDT.

ROC curves obtained using MAE and MJD methods for three levels of quantization and non-quantized data are shown, in Figure 10. This figure depicts that at global false alarm probability $p_{fa} = 0.2$, the probability of detection, p_d , attains the values 0.653, 0.684 and 0.803 for the cases of three-level data transmissions with MJD, MAE and the non-quantized data transmission, respectively. Increasing the quantization level makes the MAE and MJD methods perform more closer to the performance without quantization which is depicted in Tables 1 and 2.

Table 1 shows the p_d for 2, 3, 4 and 6 level MAE and MJD based quantized and non-quantized data transmissions for the values of $p_{fa} = 0.1, 0.2, 0.3$ and 0.4. At each quantization level MAE method performs better compared to MJD and the performance increases when the quantization level is increased. At 6-level quantization p_d obtained by MAE based method is only slightly inferior to the limiting case with no quantization. Quantitatively, the difference in p_d is 0.022, 0.014, 0.018 and 0.002 for p_{fa} values of 0.1, 0.2, 0.3 and 0.4, respectively. Table 2 shows the achieved gain in p_d by using the MAE method wrt MJD method and is given by $G = (p_d^{MAE_i} - p_d^{MJD_i})$ with the resulting percentage gain $PG = (G \times 100\%) / p_d^{MAE_i}$, where $i = 2, 3, 4, 6$.

It is obviously seen from the previous tables that MAE outperforms MJD for $M \geq 2$ levels. The achieved gain of MAE wrt MJD is in average 0.0138 with a corresponding percentage gain of 2.13% for

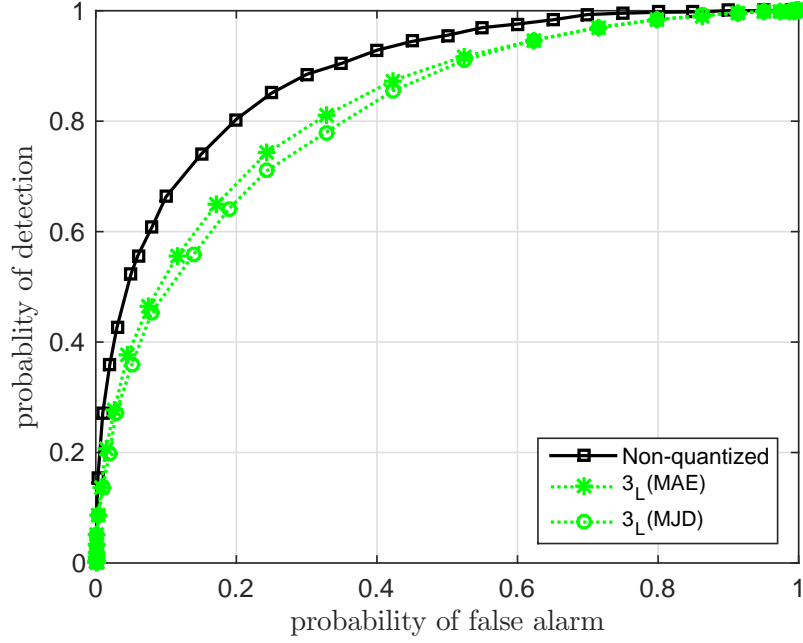


Figure 10: Comparison between the ROC curves obtained using MAE and MJD methods for three-level and Gaussian (non-quantized) DDT.

$p_d \backslash p_{fa}$	MJD ₂	MAE ₂	MJD ₃	MAE ₃	MJD ₄	MAE ₄	MJD ₆	MAE ₆	non-quantized
0.1	0.425	0.432	0.497	0.520	0.567	0.592	0.629	0.643	0.665
0.2	0.590	0.610	0.653	0.684	0.728	0.760	0.772	0.789	0.803
0.3	0.710	0.720	0.755	0.790	0.810	0.845	0.850	0.867	0.885
0.4	0.787	0.805	0.825	0.858	0.860	0.895	0.903	0.922	0.924

Table 1: The relation between p_d and p_{fa} for different levels of quantization obtained with MAE and MJD methods.

$p_d \backslash p_{fa}$	2-Level		3-Level		4-Level		6-Level	
	G	PG	G	PG	G	PG	G	PG
0.1	0.01	1.63	0.023	4.42	0.025	4.22	0.014	2.17
0.2	0.02	3.28	0.031	4.53	0.032	4.21	0.017	2.15
0.3	0.01	1.39	0.035	4.43	0.035	4.14	0.017	1.96
0.4	0.018	2.2	0.0330	3.85	0.035	3.914	0.019	2.06

Table 2: Achieved gain in p_d by using the MAE method in quantization instead of MJD.

the binary data transmissions, whereas the average gains are = 0.0305, 0.0318 and 0.0168 with corresponding average percentage gains as 4.31%, 4.12% and 2.09% for 3-level, 4-level and 6-level data transmissions, respectively. In the same manner, the average difference in p_d , for $p_{fa} = 0.1, 0.2, 0.3$ and 0.4 , between the 6-level data transmissions achieved by MAE and non-quantized data transmissions equals to 0.014 with 1.8% and it is 0.03 with 3.9% between MJD and non-quantized data transmissions. These results show that 6-level data transmission by using MAE is very close to the non-quantized data transmission and gives better performance than MJD method.

4.3 Multiple Level Data Transmission over Rayleigh Fading Channel

Figure 11 shows the ROC curves for 2, 3, 4 and 6 level MAE based quantized and non-quantized data transmissions by using M -FSK modulation scheme with non-coherent demodulation over Rayleigh fading channels and the optimal fusion rule in (7). The threshold, η , for each p_{fa} was estimated by running a Monte Carlo simulation under no event case. In this figure we can see that the obtained, p_d for 6-level quantization falls behind the limiting case of no quantization by 0.09 at $p_{fa} = 0.1$. This gain diminishes at $p_{fa} = 0.7$. When we compare the performances of different quantization levels, the achieved gain in p_d by transmitting 6-level quantization instead of 2-level quantization is 0.21 for $p_{fa} = 0.1$ and this gain diminishes at $p_{fa} = 0.99$. Also, the sub-optimal fusion rule in (15) have been used to find the ROCs for the different type of data transmissions. Figure 12 shows a comparison between the optimal and sub-optimal fusion rule for 2 and 6 levels data transmissions and compare them with the non-quantized data transmissions. The dashed line in ROCs for the sub-optimal fusion rule correspond to randomization in the tests (p.22-29) [38]. This figure shows that the achieved gain by using the optimum fusion rule wrt the sub-optimal rule is 0.3 and 0.6 at $p_{fa} = 0.1$ for the 2-level and 6-level data transmissions, respectively.

5 Conclusion

In this study we have proposed quantizing the sensor outputs by maximizing their average information in the cases of presence and non-presence of an event in decentralized detection.

The general approach in quantization for decision processes is based on distance measures such as JD and Bhattacharyya distance. This fact may have prevented a popular information based quantization criterion for decision processes maximizing the information under both (all) hypotheses rather than the information in the difference of the distributions. Since among the distance measure based quantization approaches, JD is an information theoretic quality, we adopted JD for comparisons of the proposed method.

One reason of suggesting another method like MAE instead of MJD is the non-symmetric nature of the considered problem and the fact that the advantage of Ali-Silvey type criteria [21] which MJD is a member of, is only valid for the symmetric performance measure probability of error. Although maximizing the transferred information under each hypothesis as proposed by the MAE method is a conceptually different approach, we showed that average entropy and JD are actually positively proportional quantities. This means that one might expect comparable performances using either of them for determining the quantization levels which was indeed the observation in the simulation results.

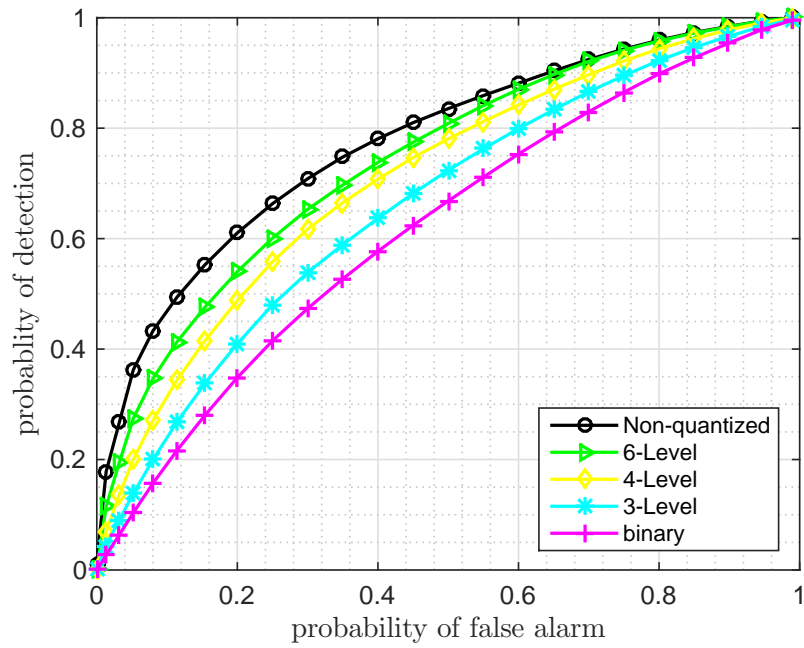


Figure 11: ROC curves in the case of fading channel by using MAE based quantization and optimum fusion rule.

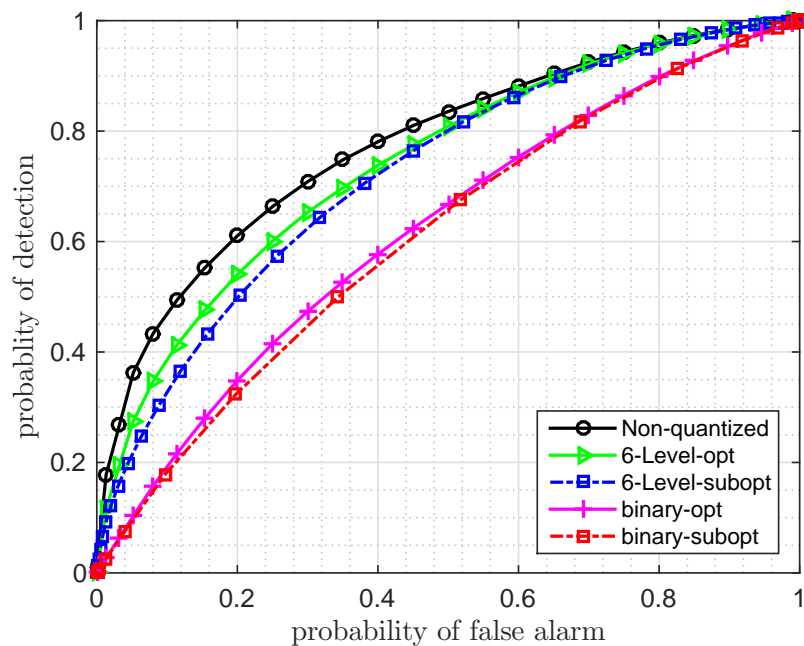


Figure 12: A comparison between the ROCs of the optimal and sub optimal fusion rule for binary and six level and its corresponding non-quantized data transmissions in the case of fading channel.

In order to isolate the effects of how the sensor outputs are quantized on the system performance we performed extensive simulation studies for the case that the sensor outputs are available error-free at the FC which we called as DDT. The performances of considered information-based methods, namely MAE and MJD, gradually improved as the quantization level was increased from binary to six-levels and it approached the performance of non-quantized data transmission. Additionally, the proposed method, MAE, performed significantly better compared to MJD for any level of quantization. Also, the effects of Rayleigh fading channel from the sensors to the FC have been investigated using the optimal and a suboptimal fusion rule for MAE. Due to the power efficiency and small degradation in non-coherent communication MFSK was adopted as the modulation scheme for the sensor to FC communication. Using the wireless channel model similar results were obtained as in DDT. Results with 6-level quantization were comparable to non-quantized data transmission.

This work showed that MAE is a valid and promising method in quantization for detection problems. A possible future work will be applying MAE method of quantization in M-ary detection problems.

6 Acknowledgement

Muath A. Wahdan, was supported by Türkiye Bursları/Scholarship for his Ph.D. studies at İzmir Institute of Technology.

References

- [1] J. Hill, M. Horton, R. Kling, and L. Krishnamurthy, The platforms enabling wireless sensor networks, *Communications of the ACM*, vol. 47, no. 6, pp. 41-46, Jun 2004.(Doi: 10.1145/990680.990705)
- [2] Ragam, Prashanth; Sahebraoji, Nimaje Devidas, Application of MEMS-based accelerometer wireless sensor systems for monitoring of blast-induced ground vibration and structural health: a review, *IET Wireless Sensor Systems* vol. 9, no. 3, pp. 103-109, Jun 2019.(Doi: 10.1049/iet-wss.2018.5099)
- [3] Anagha R, Vinoth BK, Scalable and sustainable wireless sensor networks for agricultural application of internet of things using fuzzy c means algorithm, *Sustainable Computing: Informatics and Systems*, vol. 22, no. 22, pp. 62-74, Jun 2019.(Doi: 10.1016/j.suscom.2019.02.003)
- [4] Lalatendu Muduli, Devi Prasad Mishra, Prasanta K. Jana, Application of wireless sensor network for environmental monitoring in underground coal mines: A systematic review, *Journal of Network and Computer Applications*, vol. 106, pp. 48-67, Mar. 2018.(Doi: 10.1016/j.jnca.2017.12.022)
- [5] M.Wahdan; M.Al-Mistarihi; M.Shurman, Static cluster and dynamic cluster head (SCDCH) adaptive prediction-based algorithm for target tracking in wireless sensor networks, *IEEE 8th International Convention on Information and Communication Technology, Electronics and Microelectronics (MIPRO)*, pp. 596-600, Croatia, 25-29 May, 2015.

- [6] A. Zanella, N. Bui, A. Castellani, L. Vangelista, and M. Zorzi, Internet of things for smart cities, *IEEE Internet of Things Journal*, vol. 1, no. 1, pp. 22-32, Feb. 2014.(Doi: 10.1109/JIOT.2014.2306328)
- [7] M. A. Al-Jarrah, A. Al-Dweik, Decision fusion in distributed cooperative wireless sensor networks, *IEEE Transactions on Vehicular Technology*, vol. 68, no. 1, pp. 797 - 811, Jan. 2019.(Doi: 10.1109/TVT.2018.2879413)
- [8] D. Ciunozzo, G. Romano, and P. Salvo Rossi, Optimality of received energy in decision fusion over Rayleigh fading diversity MAC with nonidentical sensors, *IEEE Transaction on Signal Process.*, vol. 61, no. 1, pp. 22-27, Jan. 2013.(Doi: 2013.10.1109/TSP.2012.2223694)
- [9] Stella I Johnsi, S. Radha, Investigations on distributed detection performance of Neyman-Pearson detection scheme using constructive interference technique for WSN, *IEEE International Conference on Wireless Communication and Sensor Computing (ICWCSC)*, India, 2-4 Jan. 2010.(Doi: 10.1109/ICWCSC.2010.5415889)
- [10] R. R. Tenney and N. R. Sandell, Detection with distributed sensors, *IEEE Transaction on Aerospace Electronics System*, vol. 17, no. 4, pp. 501-510, Jul. 1981.(Doi: 10.1109/TAES.1981.309178)
- [11] Z. Chair and P. K. Varshney, Optimal data fusion in multiple sensor detection systems, *IEEE Transactions on Aerospace and Electronic Systems*, vol. AES-22, no. 1, pp. 98-101, Jan. 1986.(Doi: 10.1109/TAES.1986.310699)
- [12] Tsitsiklis, J. N, Decentralized detection, *Advances in Statistical Signal Processing*, vol. 2, no. 2, pp. 297-344, 1993.
- [13] Viswanathan, R. and Varshney, P. K, Distributed detection with multiple sensors. I. fundamentals, *Proceedings of the IEEE*, vol. 85, no. 1, pp. 54-63, Jan. 1997.(Doi: 10.1109/5.554208)
- [14] Blum, R. S., Kassam, S. A. and Poor, H. V, Distributed detection with multiple sensors.II. Advanced topics, *Proceedings of the IEEE*, vol. 85, no. 1, pp. 64-79, Jan. 1997.(Doi: 10.1109/5.554209)
- [15] J. N. Tsitsiklis and M. Athans, On the complexity of decentralized decision making and detection problems, *IEEE Transactions on Automatic Control*, vol. 30, no. 5, pp. 440-446, May 1985.(Doi: 10.1109/TAC.1985.1103988)
- [16] V. V. Veeravalli and P. K. Varshney, Distributed inference in wireless sensor networks, *Philosophical Transactions of the Royal Society A*, vol. 370, no. 1958, pp. 100-117, Jan. 2012.
- [17] R. Viswanathan and B. Ahsant, A review of sensing and distributed detection algorithms for cognitive radio systems, *International Journal on Smart Sensing and Intelligent Systems*, vol. 5, no. 1, pp. 177-190, Mar. 2012.
- [18] Z. Zhang, A. Pezeshki, W. Moran, S. D. Howard, and E. K. P. Chong, Error probability bounds for balanced binary relay trees, *IEEE Transactions on Information Theory*, vol. 58, no. 6, pp. 3548-3563, Jun. 2012.(Doi: 10.1109/TIT.2012.2187323)

- [19] Z. Zhang, E. K. P. Chong, A. Pezeshki, W. Moran, and S. D. Howard, Submodularity and optimality of fusion rules in balanced binary relay trees, *IEEE 51st Conference on Decision and Control (CDC)*, pp. 3802–3807, 10-13 Dec. 2012.(Doi: 10.1109/CDC.2012.6427057)
- [20] B. G. Gagyasi, Distributed detection in wireless sensor networks, Ph.D. dissertation, Department of electrical engineering, Indian Institute Technology., Mumbai, India, 2008.
- [21] H. V. Poor and J. B. Thomas, Applications of Ali-Silvey distance measures in the design of generalized quantizers, *IEEE Transactions on Communications*, vol.25, no. 9, pp. 893-900, Sep. 1977.(Doi: 10.1109/TCOM.1977.1093935)
- [22] H. V. Poor, A companding approximation for the statistical divergence of quantized data, *IEEE 22nd Conference on Decision and Control*, San Antonio, TX, Dec. 1983.(Doi: 10.1109/CDC.1983.269610)
- [23] H. V. Poor, Fine quantization in signal detection and estimation-Part 1, *IEEE Transactions on Information Theory*, vol. 34, no.5, pp. 960-972, Sep. 1988.(Doi: 10.1109/18.21219)
- [24] C. C. Lee and J. J. Chao, Optimum local decision space partitioning for distributed detection, *IEEE Transaction on Aerospace Electronics System*, AES,vol. 25, no. 7, pp. 536-544, Jul. 1989.(Doi: 10.1109/7.32086)
- [25] D.J. Warren and P.K. Willett, Optimum quantization for detector fusion: some proofs, examples, and pathology, *Journal Franklin Institute*, vol. 336, pp. 323-359,Mar. 1999.
- [26] C. Altay and H. Delic, Optimal quantization intervals in distributed detection, *IEEE Transaction on Aerospace Electronics System*, vol. 52, no. 1, pp. 38-48, February 2016.(Doi: 10.1109/TAES.2015.140551)
- [27] B. Chen, R. Jiang, T. Kasetkasem, and P. K. Varshney, Fusion of decisions transmitted over fading channels in wireless sensor networks, *IEEE 36th Asilomar Conference on Signals, Systems and Computers*, Pacific Prove, CA, 2002.(Doi: 10.1109/ACSSC.2002.1196970)
- [28] B. Chen, R. Jiang, T. Kasetkasem, and P. K. Varshney, Channel aware decision fusion in wireless sensor networks, *IEEE Transactions on Signal Processing*, vol. 52, no.12, pp. 3454–3458, Dec. 2004.(Doi: 10.1109/TSP.2004.837404)
- [29] B. Chen and P. K. Willet, On the optimality of the likelihood-ratio test for local sensor decision rules in the presence of nonideal channel, *IEEE Transactions on Information Theory*, vol. 51, no.2, pp. 693–699, Feb. 2005.(Doi: 10.1109/TIT.2004.840879)
- [30] N. Ruixin, B. Chen, and P. K. Varshney, Fusion of decisions transmitted over Rayleigh fading channels in wireless sensor networks, *IEEE Transactions on Signal Processing*, vol. 54, no.3, pp. 1018-1027, Mar. 2006.(Doi: 10.1109/TSP.2005.863033)
- [31] Jayesh H. Kotecha, V. Ramachandran, A.M. Sayeed, Distributed multitarget classification in wireless sensor networks, *IEEE Journal on Selected Areas in Communications*, vol. 23, no. 4, pp. 703-713, Apr. 2005.(Doi: 10.1109/JSAC.2005.843539)

- [32] A. Jeremic, Kon Max Wong, Bin Liu, Optimal distributed detection of multiple hypotheses using blind algorithm, IEEE Transactions on Aerospace and Electronic Systems, Volume: 47, no.1, Jan. 2011.(Doi: 10.1109/TAES.2011.5705678)
- [33] N. Maleki and A. Vosoughi, Channel-aware m-ary distributed detection: Optimal and sub-optimal fusion rules, IEEE Statistical Signal Processing Workshop (SSP), 5-8 Aug. 2012.(Doi: 10.1109/SSP2012.6319783)
- [34] Z.Hajibabaei and A.Vosoughi, Impact of wireless channel uncertainty upon M-ary distributed detection systems, IEEE 25th Annual International Symposium on Personal, Indoor, and Mobile Radio Communication (PIMRC), Washington, DC, USA, 2-5 Sept. 2014.(Doi: 10.1109/PIMRC.2014.7136253)
- [35] D. G. Messerschmitt, Quantizing for maximum output entropy, IEEE Transactions on Information Theory, vol.17, no.5, p. 612, Sep. 1971.(Doi: 10.1109/TIT.1971.1054681)
- [36] M. Wahdan and M. Altinkaya, "Optimal quantization in decentralized detection by Maximizing the Average Entropy of the Sensors," IEEE 27th Signal Processing and Communications Applications Conference (SIU), p. 612, Sivas, Turkey, 24-26 Apr. 2019.(Doi: 10.1109/SIU.2019.8806534)
- [37] Bercher J.F, Vignat C., Estimating the entropy of a signal with applications, IEEE Transaction on Signal Processing, vol.48, no.6, p.1687 - 1694, Jun 2000.(Doi: 10.1109/78.845926)
- [38] H. V. Poor, An Introduction to signal detection and estimation, New York, NY, USA: Springer-Verlag, 1988.